

LA-UR-22-27535

Approved for public release; distribution is unlimited.

Title: Magnetic-Field Diffusion Effects in Beam Position Monitors II:
Application to Calibration Single-Pulse Data

Author(s): Broste, William B.
Ekdahl, Carl August Jr.
Johnson, Jeffrey B

Intended for: Report

Issued: 2022-07-27



Los Alamos National Laboratory, an affirmative action/equal opportunity employer, is operated by Triad National Security, LLC for the National Nuclear Security Administration of U.S. Department of Energy under contract 89233218CNA00001. By approving this article, the publisher recognizes that the U.S. Government retains nonexclusive, royalty-free license to publish or reproduce the published form of this contribution, or to allow others to do so, for U.S. Government purposes. Los Alamos National Laboratory requests that the publisher identify this article as work performed under the auspices of the U.S. Department of Energy. Los Alamos National Laboratory strongly supports academic freedom and a researcher's right to publish; as an institution, however, the Laboratory does not endorse the viewpoint of a publication or guarantee its technical correctness.

Magnetic-Field Diffusion Effects in Beam Position Monitors II: Application to Calibration Single-Pulse Data

William B. Broste, Carl A. Ekdahl, and Jeffrey B. Johnson

Abstract—Beam position monitors (BPMs) provide time-resolved measurements of the current and centroid position of high-current electron beams in linear induction accelerators (LIAs). One of the types of detectors used in BPMs is the B-dot loop, which generates a signal from the EMF due to the time varying magnetic flux through the loop. If some of the boundaries of the loop are composed of thick metal walls with finite conductivity, the resulting signal must be corrected for the magnetic field diffusion into the metal. From first principles, we have derived the perturbation to BPM measurements due to this effect. The theoretical framework was used to design an algorithm for signal correction that does not require knowledge of the time history of the magnetic flux being measured. Corrected signals based on that process compared favorably with the known reference signals in a laboratory calibration test sequence.

Index Terms—Linear induction accelerators, electron-beam diagnostics, current measurements, beam position monitors, magnetic diffusion

I. INTRODUCTION

FLASH radiography is often used as a diagnostic of explosively-driven experiments. For the largest of these experiments, an intense relativistic electron beam (IREB) is focused onto a target of high-Z metal to create the source spot for point-projection radiography [1]. Linear induction accelerators (LIA) are often used to create the IREB for this diagnostic technique. In the United States, three LIAs are presently used for this purpose [2], and a fourth, called Scorpius, is under development [3].

One of the most important IREB diagnostics for tuning these LIAs to produce radiographic quality beams are the beam position monitors (BPMs) that provide time-resolved measurements of the beam current and the position of the beam centroid. For our high-current LIAs, BPMs based on detection of the beam magnetic field have proven to be very effective and reliable [4, 5]. The field detector of our new BPMs under development for Scorpius is the B-dot loop shown in Fig. 1. This geometry is sometimes referred to as an “inductive shunt” [6] or “groove monitor.”

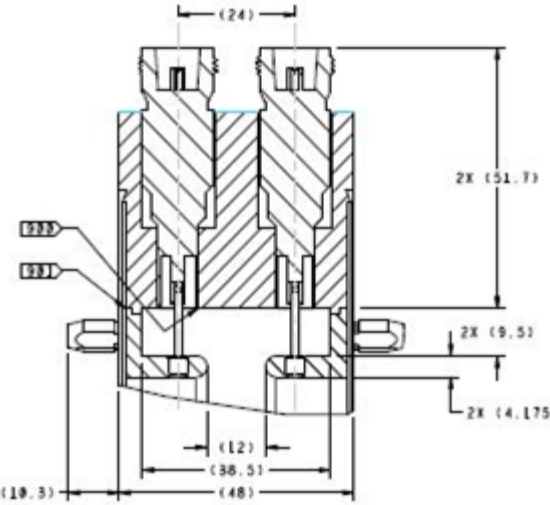


Fig. 1: Cross-section of BPM. Sensing area between the coax pin and the walls is bounded by $\Delta r = 0.95$ cm and $\Delta \ell \approx 0.725$ cm.

If the material of the walls were perfectly conducting, the EMF signal would be given by Lenz’s law

$$\begin{aligned} \mathcal{E}_0 &= -\frac{\partial \Phi_0}{\partial t} \\ &\approx -A_c \frac{\partial B_{\theta 0}}{\partial t} \end{aligned} \quad (1)$$

where A_c is the nominal area of the sensing loop.

If the cavity walls have finite conductivity, the magnetic flux will diffuse into the material, so the EMF sensed by the pin will be

$$\mathcal{E} = -\frac{\partial}{\partial t} [\Phi_0 + \delta\Phi] \quad (2)$$

where $\delta\Phi$ is the flux due to the diffused field, and integrating one has

$$\Phi = \Phi_0 \left[1 + \frac{\delta\Phi}{\Phi_0} \right] \quad (3)$$

and if the diffusion term is small enough, one has

$$B_\theta \approx -\frac{\Phi_0}{A_c} \left[1 + \frac{\delta\Phi}{\Phi_0} \right] \quad (4)$$

Therefore, to correct the integrated data, one must subtract $\delta\Phi / \Phi_0$.

A derivation of the value of the measured signal $B_m(t)$ for a known input of $B_0(t)$ has been presented in a recent paper [7] and presents convincing evidence of the validity of the fundamental diffusion equations as applied to the Scorpius BPM geometry. However, use of the BPM on an LIA requires the ability to determine $B_0(t)$ starting from $B_m(t)$. From [7],

$$B_m(t) = B_0(t) + \frac{1}{\sqrt{t_D}} \int_0^t \frac{B_0(\tau)}{(t-\tau)^{1/2}} d\tau \quad (5)$$

and determining $B_0(t)$ becomes a matter of solving the integral equation. While one of the authors was pursuing the work reported in [7], another was pursuing an alternate approach which is presented in what follows.

II. INTEGRAL FORMULATION OF DIFFUSION

From the theory discussion in [7] the total flux sensed by one of the BPM loops when a step function field is initiated at time zero is

$$\Phi(t) = \Phi_0 \left[1 + \sqrt{t/t_D} \right] \quad (6)$$

where the characteristic diffusion time t_D involves loop geometry and wall material properties.

This equation forms the basis for an alternate approach to calculating the field diffusion correction which was demonstrated prior to the Green's Function approach and its excellent results in [7]. The real benefit of this form of the diffusion solution was that experimenting with its application provided the clue to determining a correction without having to solve the integral equation for $B_0(t)$.

III. APPLICATION TO A KNOWN INPUT PULSE

Verification of the validity of equation (6) was carried out using data obtained during the initial calibration of the Scorpius Type 1 BPM. [8] Very early in the process of seeking a correction for the diffusion in the Scorpius prototype BPMs, it was observed that the superposition of equation (6) and its negative, displaced by a time T (producing the diffused results for an input square wave of length T) produced a correction term which could be subtracted from the measured flux. The signal corrected in that way was a good, though less than ideal in detail, reproduction of the calibration reference signal. The next step in the evolution of this approach was to use a superposition of a series of square wave

functions to approximate the known input. The correction flux computed for each of the square waves could then be summed to form the desired correction term to be removed from the measured data. Figure 2 illustrates a ten layer square wave approximation to the reference pulse

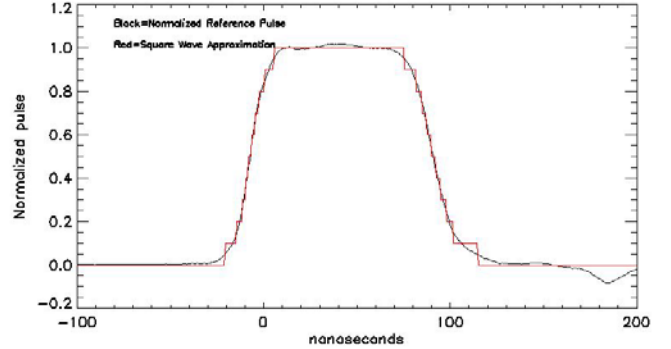


Figure 2. Reference pulse and multiple square wave approximation. Black Curve: Reference pulse normalized across flat top. Red Curve: Sum of square waves used to compute diffusion correction.

. For the well-behaved calibration source pulse, this ten layer representation was used to calculate the corrected pulse shown together with the uncorrected input and the reference pulse shape in Figure 3.

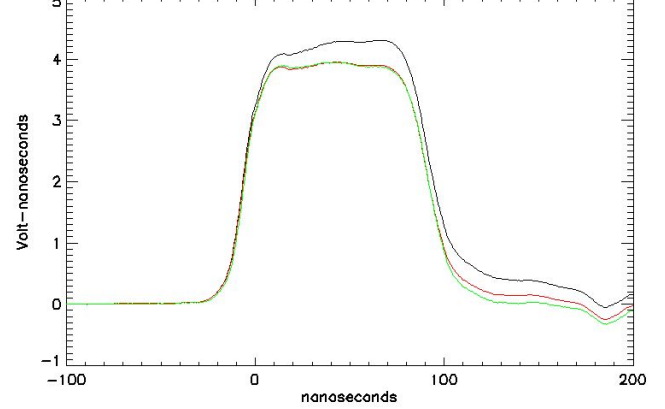


Figure 3. Comparison of b -dot output and its correction. Black Curve: Raw data. Red Curve: Data after correction for diffusion using ten- layer square wave approximation. Green Curve: Reference pulse normalized to corrected data over pulse top.

While the basic theory provides a value for the diffusion amplitude for an ideal sensing loop based on average material properties, the correlation of details between the corrected data and the reference was used to adjust the diffusion constant within realistic limits to achieve the result shown.

IV. EXTENSION TO A GENERAL CASE

Once the validity of the integral formulation for the diffusion correction was established using the known undiffused field time history based on the calibrator reference signal, the next step was to test the possibility of achieving a similarly accurate correction without using the known input.

The key to this approach came from two observations during the computations involving the known source: First, a single square wave approximation to the pulse yielded a first-order corrected pulse that matched the reference shape within 1.5% on the relatively flat top portion of the pulse. Second, using the first order corrected pulse shape as the source in the multi-layer computation produced final corrections that were indistinguishable from using the known reference pulse as the source in the multi-layer computation. That result is not surprising, because as long as the pulse being corrected is well behaved (no discontinuities, or large second derivatives) the final correction using the first order correction as a starting point should be correct to better than second order in the correction. For the $\sim 10\%$ diffusion observed in the Scorpius BPM for the 100ns pulse, better than second order implies less than 1% error in the pulse amplitude after correction.

The two step approach was implemented by searching the diffused pulse for the 80% of peak value on the rising and falling edges, then using those points as limits for the square wave used to calculate the first order correction. After applying that correction to the raw data, the first-order corrected data was then approximated by ten layers, following the prescription developed for computation of the correction using the known input shape. The final correction was then computed as the sum of the ten square wave step corrections. Figure 4 presents the results of that calculation, showing the measured waveform, first order corrected waveform, and the final second order corrected waveform, with the reference pulse from the calibration test as the fourth trace on that figure.

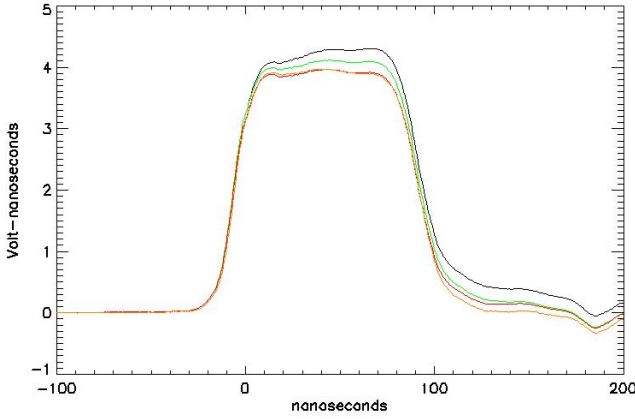


Figure 4. Two-stage diffusion correction. Black Curve: Uncorrected data for a single b-dot. Green Curve: First order correction of raw data. Red Curve: Final diffusion corrected data. Gold Curve: Reference pulse normalized to corrected data on flat top.

The normalization of the reference pulse to the corrected data provides the absolute sensitivity calibration for this b-dot. There is a small discrepancy between the corrected and reference traces in the early part of the return to baseline values, but the agreement across the top of the pulse suggests that the calibration accuracy should be better than $\pm 5\%$.

V. USE ON A CALIBRATION DATA SET

Achieving the correction shown in Figure 4 for a single trace was satisfying, but broader experience with the correction process was necessary to provide a higher level of confidence in its use. All of the BPM's in use on the DARHT LIA's were calibrated according to a standard protocol using the coaxial line described in [7] and [8]. In that protocol, thirteen data sets were taken of the eight outputs of the four pairs of b-dots located at 90 degree azimuthal separation in the BPM spool with the current carrying center conductor centered in the spool. The pulse used for development of the diffusion correction process described in this paper was one of 104 such traces. In standard usage, the thirteen on-center shots provide the data for current sensitivity calculation, and an additional sixteen shots with the center conductor at off-axis locations provide for calculation of the detector position calibration. The Scorpius prototype BPM spool was installed in the DARHT BPM test stand and the standard set of data was obtained. The software used for over twenty years to process that data was carefully modified to use the two-step process outlined herein to correct the traces for diffusion before subjecting them to normal processing. The outcome of that process is a sensitivity value for each b-dot pair obtained from a fit of the b-dot traces to the calibrated reference standard. The mean value of the fitting ratio provides the calibration value, and the standard deviation of the difference between the calibrated b-dot pair and the reference provides an estimate of the accuracy of the calibration. An output for the fitting process for one of the shots in the calibration of the Scorpius prototype is shown in Figure 5.

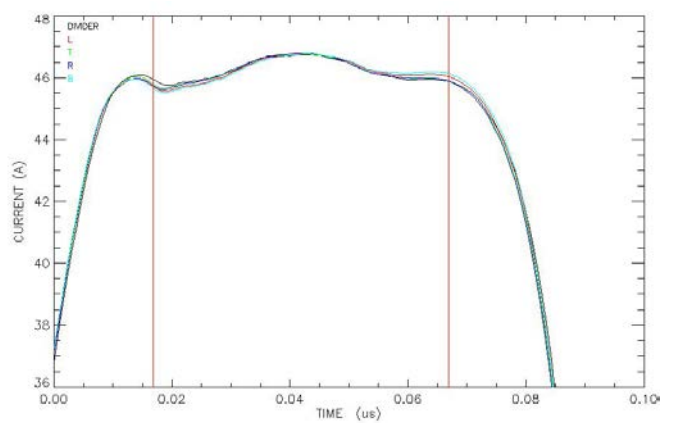


Figure 5. Expanded scale plot of fitting diffusion corrected data to calibration reference. Black Curve: Reference pulse. Red, Green, Blue and Chartreuse Curves: Diffusion corrected data for Left, Top, Right and Bottom BPM B-dot Pairs.

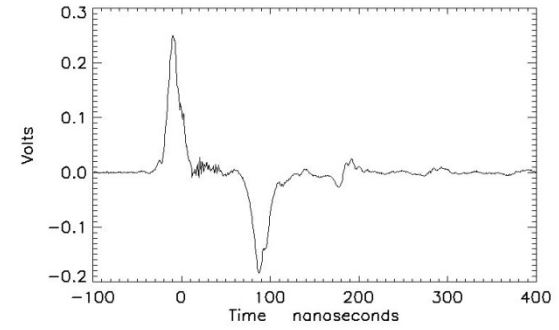
The fit and standard deviation are done for the region between the vertical red bars. For the full Scorpius data set, the standard deviation for a single detector pair on a single shot ranged from 4 to 24 out of a calibration factor of 6000 Amps/volt-microsecond, while the standard deviation of the mean value for the thirteen shots was 25 out of 6000. The four parts/thousand variance is consistent with the estimate given earlier of less than .5% uncertainty for the diffusion correction process.

VI. A USER'S GUIDE TO DIFFUSION CORRECTION

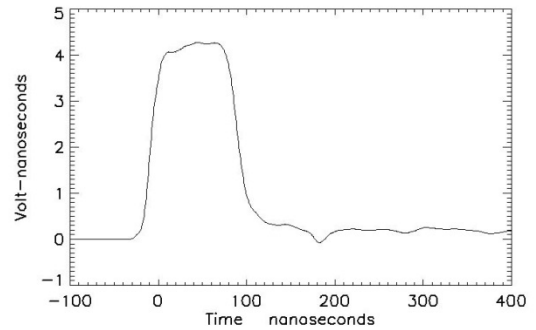
The process of calculating an integrated B-dot signal free of field diffusion effects as documented in this report has been implemented as a modification to the IDL codes used for processing BPM calibrations and data for DARHT-II. The most basic BPM calibration involves the correction of 232 traces with nine intermediate results per trace. Looking ahead to Scorpius, there is the possibility of data from twenty BPMs arriving in bursts of twenty shots every ten minutes. Displaying all the steps in the correction process (more than 25000 every twenty minutes) in those applications would be impossibly time consuming and guaranteed to produce terminal ennui in the analyst using them. However, an appreciation of the steps involved is essential to providing confidence in the process, and the ability to modify and improve it. With that in mind, the series in Figure 6 provides a recap of the process for one b-dot in the final shot of the calibration set used in the evolution of the diffusion correction method. In order, they illustrate: a) raw data; b) Integrated raw data; c) the square wave approximation used to calculate the first order correction; d) the first order correction; e) data after first order correction; f) identification of limiting points on e) for defining the next step; g) square wave layers used for computing final correction; h) final correction flux to be subtracted from b); i) a comparison of raw data (black), first order corrected data (green), final corrected data (red), and the final correction flux (blue). To assist potential users in their understanding and improvement of the process, the Appendix contains a listing of the IDL code diffusiongen.pro as installed in the calibration and DARHT-II data analysis codes modified for dealing with Scorpius prototype BPM data. The code should be viewed as a work-in-progress beta test, subject to continuing correction and refinement.

Figure 6. Processing Steps in Diffusion Correction. See Text for descriptions

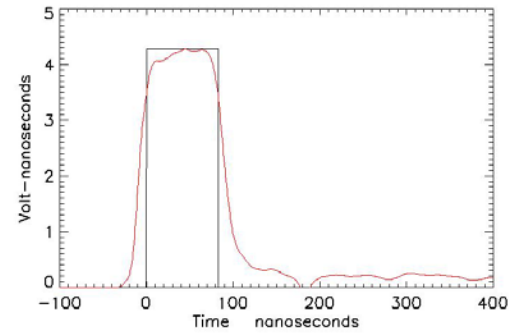
a)



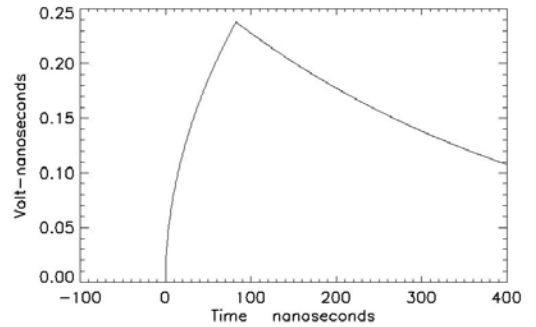
b)



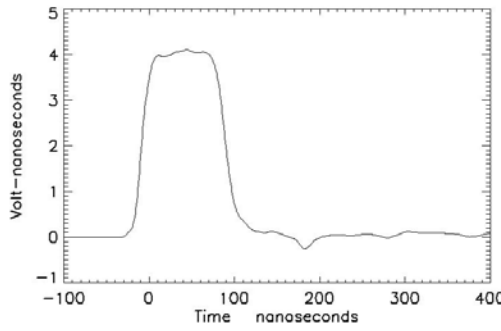
c)



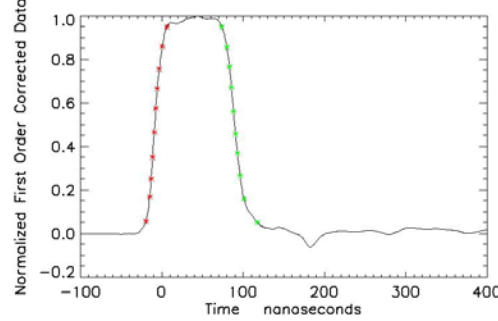
d)



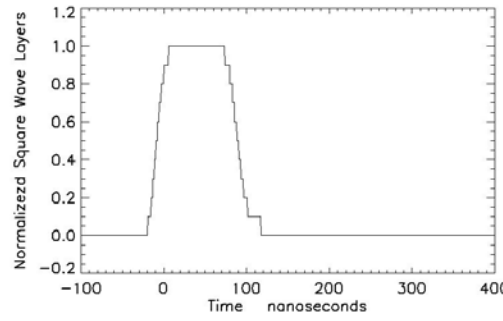
e)



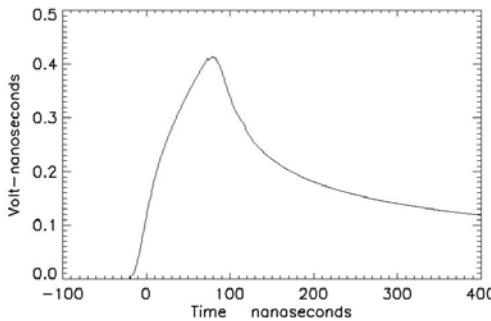
f)



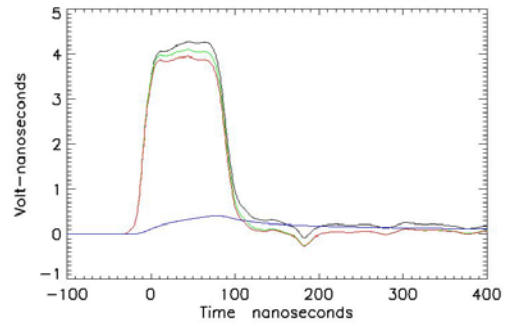
g)



h)



i)



VII. CONCLUSION

We have derived an expression for the time varying flux due to diffusion of magnetic field into the metal walls of the Scorpius BPMs. Correction of measured data with that calculated diffusion yields an undiffused result in good agreement with experimental measurements. When carefully applied to BPM calibration data, the correction process leads to BPM sensitivity factors which can be used to make accurate measurements of LIA current and position. Application of the correction process and the calibration factors thus derived, to BPM data acquired from a relativistic electron beam experiment will be discussed in a following paper. Extension of the technique to multipulse data is also forthcoming.

ACKNOWLEDGMENT

The authors wish to thank their colleagues at Los Alamos and elsewhere for years of stimulating discussions about this, and other physical phenomena topics.

This work was supported by the U.S. Department of Energy through the Los Alamos National Laboratory. Los Alamos National Laboratory is operated by Triad National Security, LLC, for the National Nuclear Security Administration of U.S. Department of Energy (Contract No. 89233218CNA000001).

REFERENCES

- [1] K. Peach and C. Ekdahl, "Particle radiography," *Rev. Acc. Sci. Tech.*, vol. 6, pp. 117 - 142, 2013.
- [2] C. Ekdahl, "Modern electron accelerators for radiography," *IEEE Trans. Plasma Sci.*, vol. 30, no. 1, pp. 254-261, 2002.
- [3] M. T. Crawford and J. Barraza, "Scorpius: The development of a new multi-pulse radiographic system," in *Proc. 21st IEEE Int. Conf. Pulsed Power*, Brighton, UK, 2017.
- [4] C. Ekdahl, E. O. Abeyta, H. Bender, W. Broste, C.

Carlson, L. Caudill, K. C. D. Chan, Y.-J. Chen, D. Dalmas, G. Durtschi, S. Eversole, S. Eylon, W. Fawley, D. Frayer, R. Gallegos, J. Harrison, E. Henestroza, M. Holzscheiter, T. Houck, T. Hughes, S. Humphries, D. Johnson, J. Johnson, K. Jones, E. Jacquez, B. T. McCuistian, A. Meidinger, N. Montoya, C. Mostrom, K. Moy, K. Nielsen, D. Oro, L. Rodriguez, P. Rodriguez, M. Sanchez, M. Schauer, D. Simmons, H. V. Smith, J. Studebaker, R. Sturgess, G. Sullivan, C. Swinney, R. Temple, C. Y. Tom and S. S. Yu, "Initial electron-beam results from the DARHT-II linear induction accelerator," *IEEE Trans. Plasma Sci.*, vol. 33, no. 2, pp. 892 - 900, 2005.

[5] J. Johnson, C. Ekdahl and W. Broste, "DARHT axis-II beam position monitors," in *AIP Conference Proceedings*, vol. 732(1), 2004.

[6] C. Ekdahl, "Voltage and current sensors for a high-density Z-pinch experiment," *Rev. Sci. Instrum.*, vol. 51, no. 12, pp. 1845 - 1848, 1980.

[7] Carl Ekdahl, William Broste and Jeffrey Johnson, "Magnetic-Field Diffusion Effects in Beam Position Monitors I: Theory" LA-UR-22-26981, 2022

[8] Jeffrey B. Johnson and Kip A. Bishofberger, "Initial Testing of the Scorpius Beam Position Monitors", LA-UR-21-28704 Scorpius -TN-099, 2021

APPENDIX

IDL Code for Diffusion Correction of Integrated B-dot Data

```

pro diffusiongen,sign,traw,draw,dfixed
;Latest update 16 July 2022
;This is the concatenation of routines to perform diffusion correction without
;a known source function. Installed in bdot_cal_scorpius4 and ASD_bdot_220703
;diagnostic print and plot removed prior to insert in bdot_cal,
;Contrast to bdot_cal_scorpius3 where the input shape is known from the pulse reference
;Details of philosophy and choices may be found in earlier diffusion codes
;traw and draw are integrated time and data, droop corrected
;sign is +1 or -1 depending on whether this is a positive or negative b-dot signal
draw=sign*draw
dettype='wresistors'
;set analysis parameters depending on Type 1 operating mode Ratio is used in stage 1, diffamp
in stage 2
if dettype eq 'wresistors' then ratio=1.054
if dettype eq 'noresistors' then ratio=1.076
if dettype eq 'wresistors' then diffamp=.090
if dettype eq 'noresistors' then diffamp=.130

npts=n_elements(traw)
dt=(traw(npts-1)-traw(0))/(npts-1)
maxrawint=MAX(draw,maxintsubscript)
;find the 80% of max point on rise and the 80% max point on fall
lolimit=npts/2 ;assumes the max is after the mid point of the record
;from early new BPMTS work, not a guarantee. Move 500 points earlier just to be safe
lolimit=lolimit-500
hilimit=maxintsubscript
;find time and value for 80% of max on rising edge
level=.8*maxrawint
k=1
while draw(lolimit+k)lt level do k=k+1
starttime=traw(lolimit+k)
startlevels=draw(lolimit+k)
startindex=lolimit+k

;find times and value for 80% of max on falling edge
k=1

```

```

while draw(hilimit+k)gt level do k=k+1
  endtime=traw(hilimit+k-1)
  endlevel=draw(hilimit+k-1)
  endindex=hilimit+k-1
;the square wave approximation will go from starttime to endtime and startindex to endindex

;set up arrays to hold first order correction
intmod=fltarr(npts)
tmod=fltarr(npts)

;THE AMPLITUDE OF THE first order CORRECTION IS SET SO INTEGRATED DATA IS REDUCED BY (ratio-1)/RATIO at 70ns
ampmod=maxrawint*((ratio-1.)/ratio)
;THIS AMPMOD WILL GIVE A CORRECTION TO BE SUBTRACTED FROM INTEGRATED DATA OF (RATIO-1)*(CORRECTION FLUX VALUE)
;AT 70 NS FROM start of correction
;That time was chosen based on early work with DARHT test stand cal pulse, as the approximate time of peak correction
;Based on experience with development using cal pulses, using a correction without rise time details and an exponential
;decay approximation gave a first-order corrected pulse that showed good fidelity to ;the final shape to 1-2% on the nominal flat top.

for i=startindex,endindex do intmod(i)=ampmod*sqrt((dt*(i-startindex))/.070)

;for the first order correction, the late relaxation is exponential with .4 microsecond time constant
latemod=fltarr(npts)
taurelax=.4
FOR i=endindex+1,npts-1 do latemod(i)=intmod(endindex)*EXP(-((i-(endindex))*dt)/taurelax)
;subtract the first order diffusion correction and latemod from raw data
DATAMOD2=draw-intmod-latemod

dmod=sign*datamod2
;this is the first order corrected data using the 80 percent square wave
;go back to positive only function
dfo=sign*dmod
;dfo is first order corrected data

;begin using the dfo as the source for computing the final correction

;10 layers are to be built from zero to the peak value of the input array dfo as it rises.

;normalize the first order so max is 1.
maxfo=MAX(dfo,maxfosubscript)
pulsnorm=maxfo
dnorm=dfo/pulsnorm

;find start and stop times and indices for 10 levels from .05 to .95 of normalized dfo
levels=fltarr(10)
starttimes=fltarr(10)
startlevels=fltarr(10)
endtimes=fltarr(10)
endlevels=fltarr(10)

for i=0,9 do levels(i)=.1*(i+.5)
hilimit=maxfosubscript
;rising limits found from nominal before zero time up to max of input

;find times and values on rising edge
for j=0,9 do begin
  k=1
  while dnorm(lolimit+k)lt levels(j) do k=k+1
  starttimes(j)=traw(lolimit+k)
  startlevels(j)=dnorm(lolimit+k)
endfor ;j

```

```

;find times and values on falling edge  start looking at maximum+1
for j=0,9 do begin
  k=1
  while dnorm(hilimit+k) gt levels(j) do k=k+1
  endtimes(j)=traw(hilimit+k-1)
  endlevels(j)=dnorm(hilimit+k-1)
endfor ;j

;modeling both up and down diffusion with the layer cake model
;signal will accumulate layers, difftotal the correction
signal=fltarr(npts)
difftotal=fltarr(npts)
time=traw
amp=.1  ;set layer thickness  ten layers taken from normalized first order

for i=0,9 do begin ; i is the layer index

;zero layer arrays
  uplayer=fltarr(npts)
  downlayer=fltarr(npts)
  signallayer=fltarr(npts)
  difflayer=fltarr(npts)
;Begin calculation of correction required for layer i
  layerstart=starttimes(i)
  layerend=endtimes(i)
  startindex=15000+long(layerstart/dt)
  endindex=15000+long(layerend/dt)
  for j=startindex, npts-1 do uplayer(j)=amp*sqrt((j-startindex)*dt)

  for j=endindex,npts-1 do downlayer(j)=amp*sqrt((j-endindex)*dt)

  for j=startindex,endindex do signallayer(j)=amp

  signal=signal+signallayer

  difflayer=uplayer-downlayer

  difftotal=difftotal+difflayer

endfor ;i=1,10
;scale difftotal from pulse amplitude 1 to pulse amplitude at endtimes(9), which is at index
15000+endtimes(9)/dt
; also the diffusion form needs to be multiplied by diffusion amplitude/sqrt(tzero), which is
diffamp/sqrt(.060)
  normindex=long(15000 + (endtimes(9)/dt))

normfactor=dfo(normindex)*diffamp/sqrt(.060)
print, normfactor

difftotal=difftotal*normfactor

dfixed=draw-difftotal
dfixed=sign*dfixed
;plot, traw, draw, xrang=[-.1,1]
;oplot, traw, dfixed, color=2
end; diffusiongen

```